Available online at www.sciencedirect.com
ScienceDirect
Journal of Solid State Chemistry 180 (2007) 2587–2596
JOURNAL OF SOLID STATE CHEMISTRY
www.elsevier.com/locate/jssc

Thermal phase transitions in antimony (III) oxides

R.G. Orman, D. Holland*

Department of Physics, University of Warwick, Coventry, CV4 7AL, UK

Received 11 May 2007; received in revised form 4 July 2007; accepted 8 July 2007
Available online 13 July 2007

Abstract

Previous reports of the thermal behaviour of antimony trioxide show significant disagreement on the values for the temperatures associated with specific thermal events. In this reappraisal, samples of both polymorphs of Sb_2O_3 (senarmontite and valentinite) have been analysed using X-ray diffraction and simultaneous differential thermal/thermogravimetric analysis techniques. The senarmontite–valentinite phase transition has been observed to occur as a multi-stage event commencing at temperatures as low as $615\pm3\,^{\circ}C$—evidence of oxidation to Sb_2O_4 under inert atmosphere may indicate that the depression is related to surface- or bulk-bound water. Valentinite produced by mechanical milling of senarmontite exhibits the reverse phase transition to senarmontite at a lower than normal temperature ($445\pm3\,^{\circ}C$). Oxidation temperatures of $531\pm4\,^{\circ}C$ for senarmontite and $410\pm3\,^{\circ}C$ for mechanically derived valentinite were also recorded.

Keywords: Antimony oxide; Phase transitions; Thermal analysis

1. Introduction

Antimony (III) oxide exists as two crystalline polymorphs: senarmontite, the low-temperature cubic form consisting of Sb_4O_6 molecules, and valentinite, an orthorhombic structure of chains of $[SbO_3]$ trigonal pyramids. Several thermal studies of these oxides have been undertaken previously, but there is significant disagreement between the values presented by different researchers for the temperatures associated with the thermal events.

On heating, senarmontite (structure shown in Fig. 1(a) [1]) undergoes a solid–solid phase transition to the high-temperature-stable valentinite form (Fig. 1(b) [2]), but the transition temperature for this event has been reported to have values in the range 556–655 °C in different studies (Table 1) [4–12]. Roberts and Fenwick [4] determined it to be $570\pm10\,^{\circ}C$, although the Sb_2O_3 used in their experiment initially had a high sulphide content and the subsequent purification process may have affected their results. Jones et al. [10] calculated a value of 650 °C from thermodynamic data before confirming experimentally that the transition occurred at or before this point. In their study of antimony oxides, Golunski et al. [5] measured the onset temperature of the transition to be 629 °C, whilst Centers [11] gave a temperature of 556 °C.

Conflicting oxidation temperatures for the two polymorphs have also been reported (Table 1), although there is general agreement that valentinite oxidises noticeably earlier than senarmontite. Of these, Golunski et al. [5] reported that valentinite did not display any mass change until ~620 °C, beyond the end of the exothermic event that they identified as being due to oxidation. Agrawal et al. [9] did not clearly specify which polymorph of Sb_2O_3 they used in their investigation, although the implication from their heat-treatments at 400 °C is that the sample was pure senarmontite. The presence of exclusively endothermic features in their study is also puzzling, since oxidation should be an exothermic event for whichever polymorph was used. Trofimov et al. [6] examined the oxidation of a mixture of the two polymorphs, noting that this began to oxidise earlier than either polymorph individually and that it was the senarmontite in the sample that reacted before the valentinite in this situation. The explanation offered for the lowered temperature was that there was coherent linking of the Sb_2O_4 (cervantite) phase (Fig. 1(c) [3]) to the original valentinite matrix, substantially reducing the

*Corresponding author. Fax: +44 24 76692016.
E-mail address: d.holland@warwick.ac.uk (D. Holland).

0022-4596/$ - see front matter © 2007 Elsevier Inc. All rights reserved.
doi:10.1016/j.jssc.2007.07.004

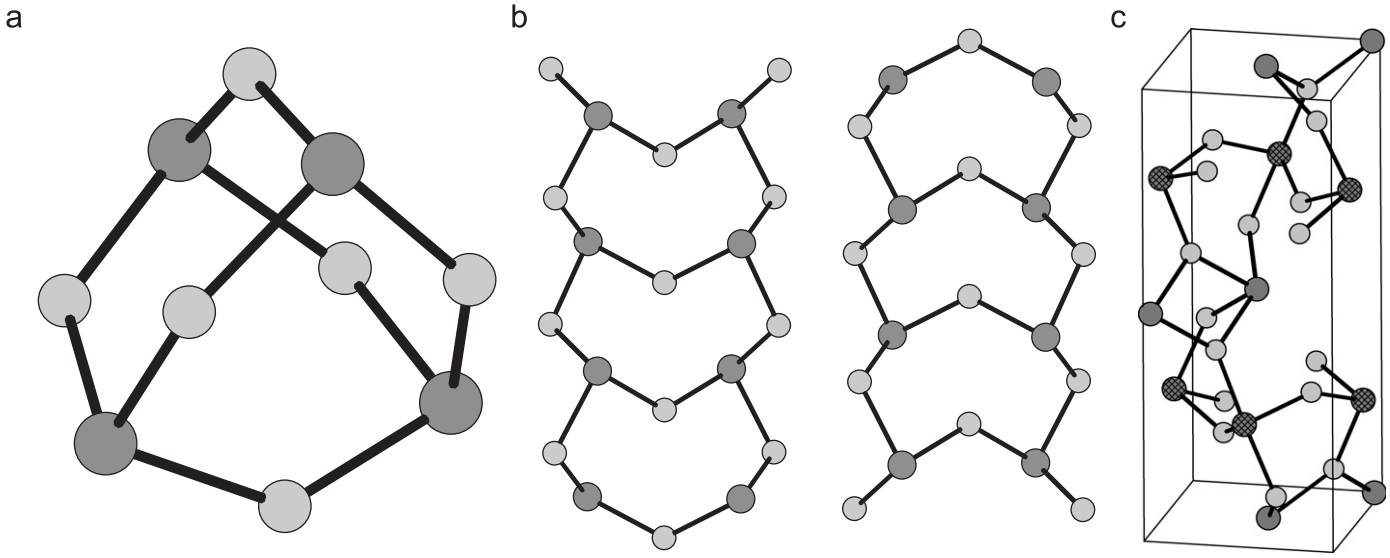

Fig. 1. The structures of (a) α-Sb_2O_3, senarmontite [1], (b) β-Sb_2O_3, valentinite [2], and (c) α-Sb_2O_4, cervantite [3]. Darker atoms are antimony, with hatching distinguishing the Sb^{5+} atoms from Sb^{3+} in the Sb_2O_4 structure.

Table 1
The phase transition and oxidation temperatures, and the changes in mass after heating, of senarmontite and valentinite, as reported by various authors

Senarmontite–valentinite transition temperature (°C)	Senarmontite oxidation temperature (°C)	Mass change in senarmontite after heating to melting point (%)	Valentinite oxidation temperature (°C)	Mass change in valentinite after heating to melting point (%)	Mixture oxidation temperature (°C)
570 ± 10 [4]	575 [5]	−26 [5]	463 [5]	−18 [5][b]	380 [6]
606 ± 5 [7]	500–660 [8]	−21 [8]	450–540 [8]	+0.8 [8]	
600 ± 10 [9]	510 [9][a]	+5.5 [9]	510 [9][a]	+5.5 [9]	
629 [5]	460 [6]		400 [6]		
640–655 [10]					
556 [11]					
606 [12]					

[a]The polymorph(s) present in this sample of Sb_2O_3 was not specified by the authors.
[b]The data published by the authors show that the mass did not change until ~620 °C.

energy of nucleation. This topotactic growth process was later described in much greater detail by Gopalakrishnan and Manohar [13], and the work of Centers [11] provided further support for the hypothesis that the oxidation of Sb_2O_3 is actually sublimation-controlled, with senarmontite subliming to low-energy valentinite nucleation sites before oxidising.

The sublimation that occurs concurrently with oxidation to Sb_2O_4 complicates the process of determining the oxidation temperature. Both Cody et al. [8] and Golunski and Jackson [14] found that senarmontite begins to sublime at approximately 502 °C, whilst valentinite was observed to start losing mass at 450 °C. Because Sb_2O_4 is stable below approximately 950 °C [5], the competing volatilisation and oxidation processes can therefore be expected to lead to different overall mass changes between the two Sb_2O_3 polymorphs.

The melting point of Sb_2O_3 is the least disputed thermal event with a general consensus that it occurs soon after the senarmontite–valentinite phase transition, with a temperature of 655 ± 2 °C [6,11] usually quoted in the literature. However, Golunski et al. [5] reported a temperature of 643 ± 2 °C in their study, whilst other authors [10] have found that melting occurred between 640 and 655 °C, depending on heating rate.

2. Experimental

2.1. Sample preparation

Commercial antimony trioxide (99.6%, Alfa Aesar) was shown to be pure senarmontite, using X-ray diffraction (XRD). This was then used as the basis for two attempts to prepare a pure valentinite sample by mechanical milling, following the method described by Berry and Ren [15]. In the first attempt, 18 g of commercial Sb_2O_3 was dry-milled, at the Open University, in a Retsch PM 400 planetary ball mill, using stainless steel balls and vials (250 ml capacity) at 200 rpm with a 1:20 powder-to-ball weight ratio. Milling was undertaken for 6 h, the time found by Berry and Ren to yield an XRD pattern for pure valentinite. The second

preparation differed in that a vibrational mill was used for the mechanical milling of the commercial trioxide over a period of 8 h.

Attempts to measure the particle size of the various samples with a laser-scattering technique were hampered by the tendency of the powders to agglomerate. However, the data that could be obtained indicated that the mean particle size of the milled samples was at most half that of the commercial powder.

2.2. X-ray diffraction

XRD patterns were obtained using a Bruker D5005 diffractometer with a constant 12 mm footprint on the sample. Unless otherwise stated, all runs were over a 2θ range of 10–70° at 0.02° increments using a CuKα radiation source at 40 kV–40 mA. Aluminium holders with a 20 mm diameter circular sample area were used and any resulting aluminium diffraction peaks present in results are labelled. An acquisition time of 5 s per angular increment was used for all samples unless otherwise noted.

2.3. Simultaneous differential thermal and thermogravimetric analysis (TG/DTA)

A PerkinElmer Diamond TG/DTA system was used for all TG/DTA measurements, using either argon or air flowing at 200 ml/min as a purge gas. When running under argon, the inert gas was allowed to flow for 30 min before the start of the thermal program, to insure that all air had been purged from the system. Sample and reference masses were typically 20–40 mg and heating rates varied from 10 to 160 °C/min; the exact atmospheric and thermal conditions for each dataset are specified. Ten data points were collected per second at all heating rates.

Quartz was chosen as a reference material because a single thermal event associated with the transformation between the α and β phases of the material occurs on both heating and cooling at an onset temperature of 574 °C [12]. The advantage of having this single-point check of the temperature scale was deemed to outweigh the potential problem posed by the (relatively small) transition peak obscuring other thermal events occurring in the sample.

3. Results

3.1. X-ray diffraction

The XRD pattern of the commercial Sb_2O_3 showed only peaks from senarmontite, with no evidence for the presence of valentinite within the detection limits of the technique (~5%, Fig. 2(a)). The XRD patterns of the mechanically milled samples showed that the antimony trioxide which had been processed in the vibrational mill remained as pure

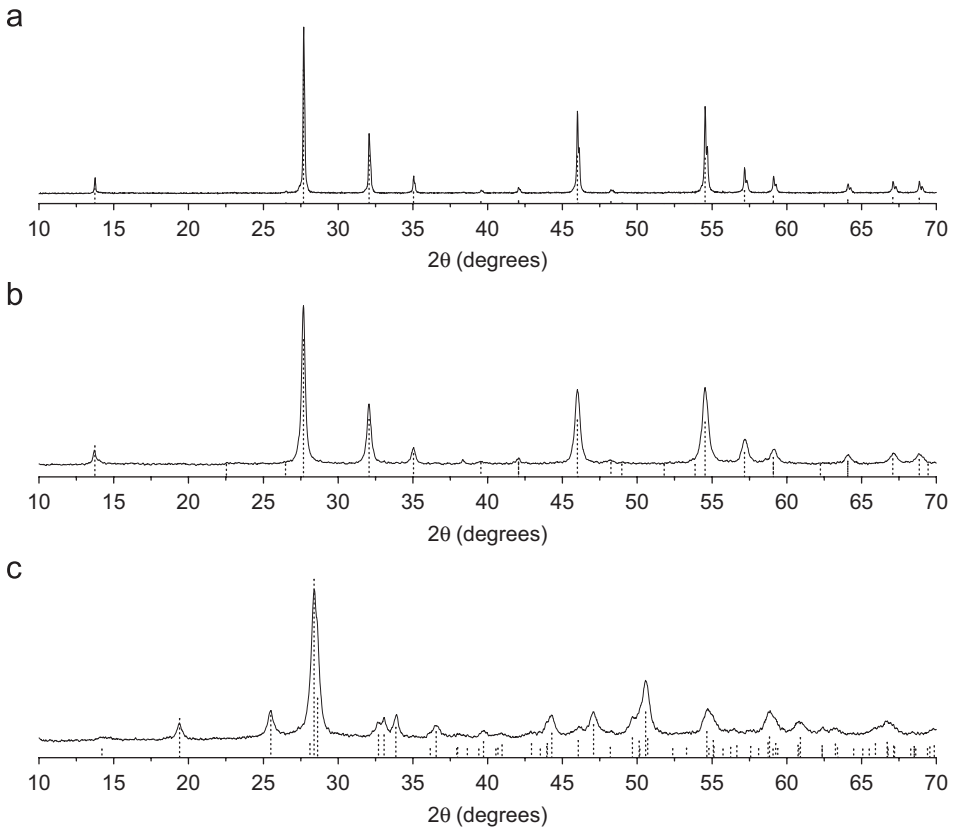

Fig. 2. XRD patterns of (a) the commercial Sb_2O_3, (b) Sb_2O_3 crushed in a vibrational mill and (c) Sb_2O_3 pulverised in a planetary ball mill. Dotted lines show the reference peaks for senarmontite in (a), (b) [1] and valentinite in (c) [2].

senarmontite (Fig. 2(b)), whilst the Sb_2O_3 from the planetary ball mill had undergone the transition to valentinite, with no diffraction peaks from senarmontite being visible (Fig. 2(c)).

3.2. Thermal analysis

3.2.1. Senarmontite

DTA data from the two senarmontite samples (commercial and mechanically milled) obtained under flowing argon are shown in Fig. 3(a) and combined DTA/TG data for commercial senarmontite are shown in Fig. 3(b). The peaks assigned to the senarmontite–valentinite transition and to melting are labelled as P and M, respectively. The peak labelled Q is due to the α–β quartz phase transition in the reference and E marks the end of the endothermic event associated with volatilisation of Sb_2O_3. Additional, unexpected events were also recorded. In the commercial senarmontite sample, event 1 has an onset of 615 ± 3 °C and peaks at 639 ± 3 °C; whilst in the mechanically milled senarmontite, feature 2 is a complex event commencing at 410 ± 5 °C under argon and at 323 ± 3 °C under air (Fig. 3(c)). A heat-treatment at 638 °C was carried out on the commercial senarmontite, in order to identify the nature of event 1, using the TG/DTA equipment in order to provide precise temperature control for a small quantity of the sample and to avoid overlap with subsequent peaks. The powder obtained by this method was spread over a flat aluminium holder for analysis by XRD over the angular range 25–35° at 0.02° increments, 75 s per step. This yielded the diffraction pattern in Fig. 4, where peaks from valentinite and cervantite can be seen, in addition to the major phase, senarmontite; the limited quantity of sample available and the method used to mount it is the likely cause of the peak shifts.

To study event 2, a DTA scan was run under argon at 20 °C/min to a temperature of 560 °C, followed by cooling; this established that the feature was both repeatable and irreversible. Samples of the milled senarmontite were subsequently heated to 250 and 520 °C, in platinum–rhodium crucibles, in a tube furnace under an argon atmosphere and held for 4 h before cooling. XRD analysis (Fig. 5) showed that the post-event 2 heat-treatment produced senarmontite with narrower peaks than the pre-event 2 heat-treatment. A separate XRD comparison of samples heat-treated in the same manner at 250 and 450 °C

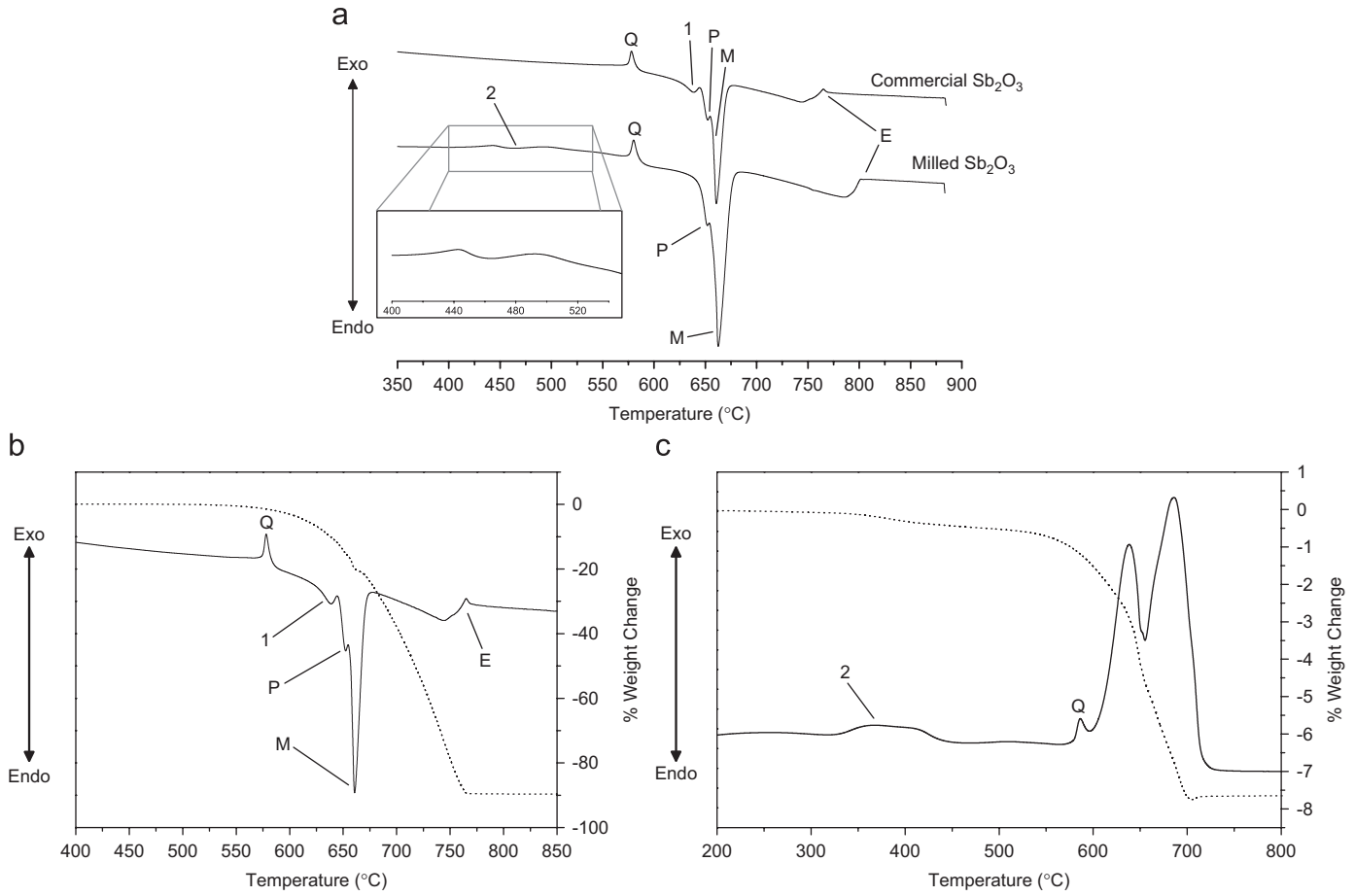

Fig. 3. Thermal data for the senarmontite samples. (a) A comparison of DTA traces at a heating rate of 20 °C/min under flowing argon. (b) DTA and TG data for the commercial senarmontite only, under the same conditions. (c) DTA and TG for the milled senarmontite sample at 40 °C/min under flowing air. TG data are the dotted lines. Peak labels are as follows: Q = α–β quartz transition; P = senarmontite–valentinite phase transition; M = melting; E = end of volatilisation. Numbered peaks are discussed in more detail in the main text.

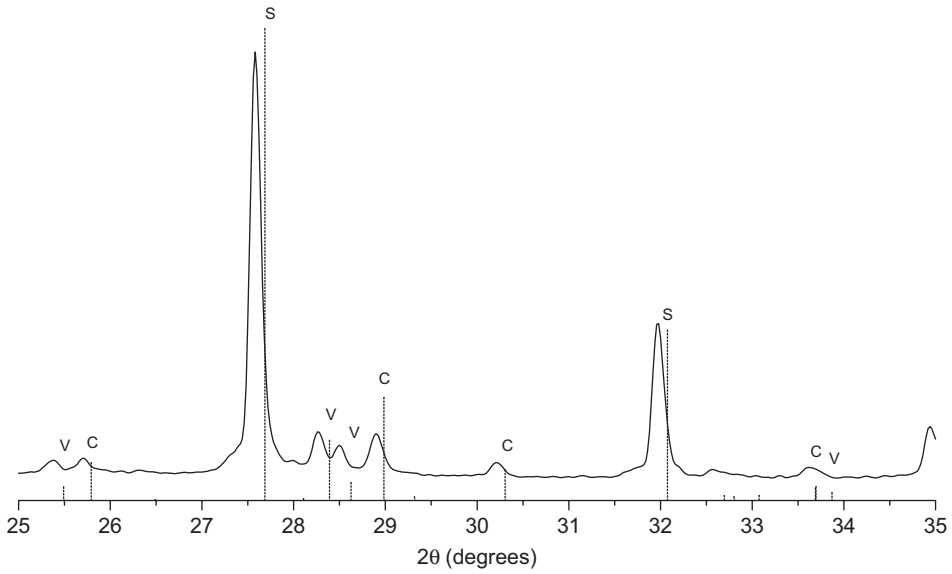

Fig. 4. The XRD pattern for the commercial senarmontite heat-treated at 638 °C under argon, compared with the primary reference peaks for senarmontite (S) [1], valentinite (V) [2] and cervantite (C) [3].

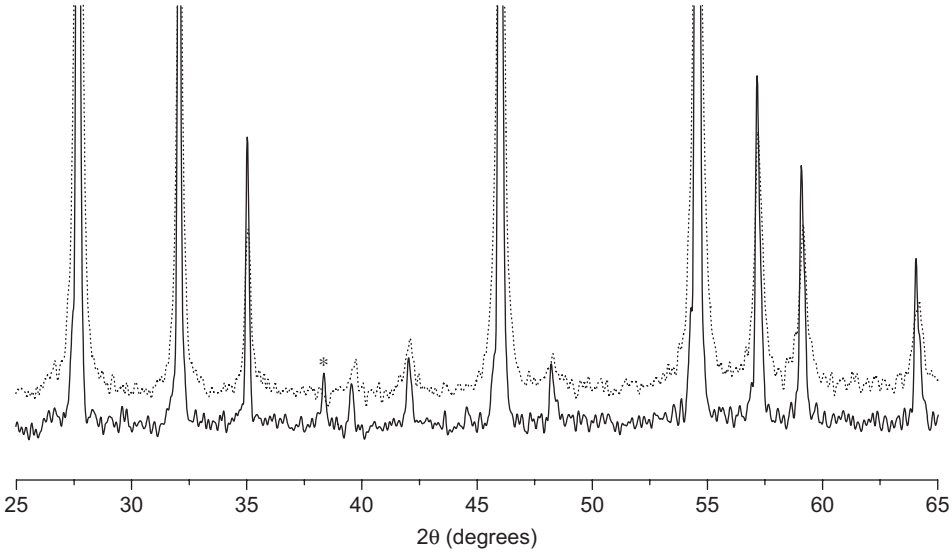

Fig. 5. Comparison of the XRD traces for the milled senarmontite sample, heat-treated at 250 and 520 °C (dotted and solid lines, respectively) under argon. The starred peak is from the aluminium holder.

under flowing air (Fig. 6) showed that some formation of cervantite occurred when the event took place in a local oxidising atmosphere but that there was no change in peak width.

Fig. 7 shows the effect of heating rate on the commercial senarmontite sample under air. It can be seen that, at higher rates, melting and other adjacent endotherms became more apparent, with oxidation effectively being suppressed—this contradicts the claim of Cody et al. that the volatilisation/oxidation temperature is "minimally" affected by heating rate [8]. Although running at a rate high enough to eliminate oxidation rendered the fine detail of the consecutive endothermic processes indistinguishable in the samples examined here, this method could be useful to access features in other oxygen-sensitive substances that would ordinarily be hidden when running under air, provided that the thermal events were well-separated.

3.2.2. *Valentinite*

The DTA trace of the mechanically derived valentinite under argon (Fig. 8) also showed additional events. The first of these, event 3, with onset at 437 ± 3 °C was investigated further by heating a sample at a point after the event had occurred (520 °C) and also by performing a DTA scan at 20 °C/min to a maximum temperature of 560 °C, followed by cooling, to determine reversibility. This latter showed that the event was irreversible and XRD analysis of the material resulting from the heat treatment revealed that the sample had completely converted to

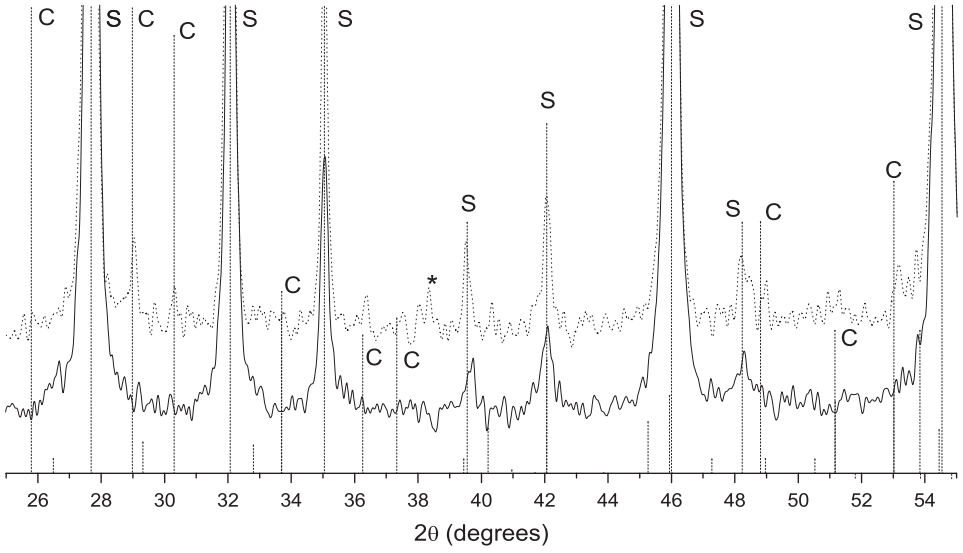

Fig. 6. Comparison of the XRD traces for the milled senarmontite sample, heat-treated at 250 and 450 °C (solid and dotted lines, respectively) under air. The starred peak is from the aluminium holder. Reference peaks for senarmontite (S) [1] and cervantite (C) [3] are also shown.

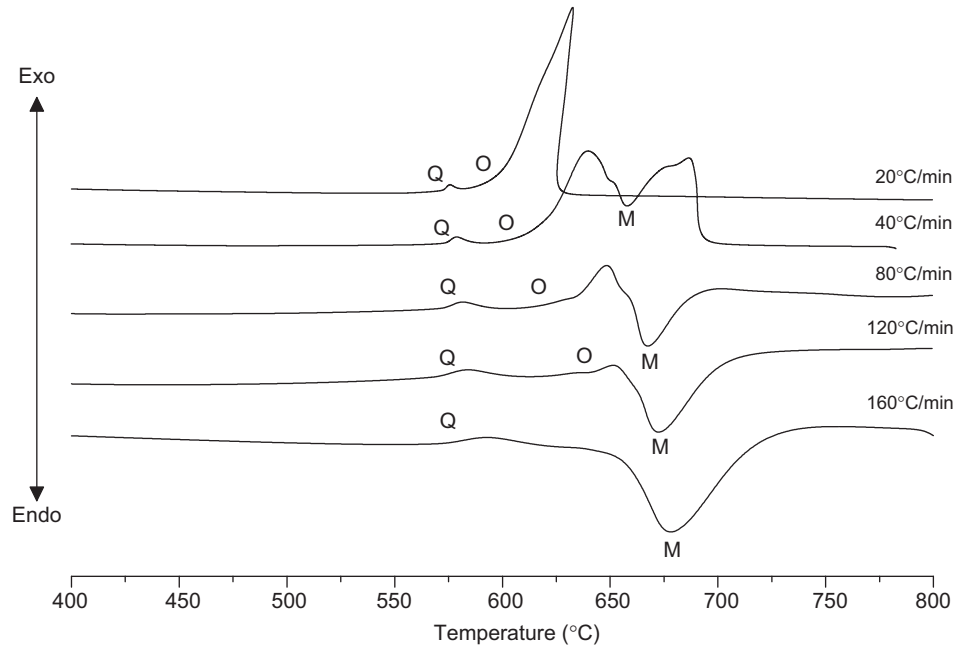

Fig. 7. Comparison of the DTA data for the commercial Sb_2O_3 sample at various heating rates under flowing air. The quartz α–β phase transition, oxidation onset and melting peaks are labelled (Q, O and M, respectively).

senarmontite. The presence of the feature under flowing air (Fig. 9) could not be confirmed due to overlap with other thermal events.

4. Discussion

4.1. Senarmontite–valentinite transition

4.1.1. Senarmontite

The endothermic event 1 at 615 ± 3 °C in the DTA trace for the commercial senarmontite (Fig. 3(a)) was unexpected since only a single pre-melting peak has been previously reported (that of the senarmontite–valentinite phase transition). The XRD analysis of the material remaining after this feature (Fig. 4) shows that it consisted principally of senarmontite, with small amounts of valentinite and cervantite (α-Sb_2O_4) also present. Although the appearance of valentinite might initially suggest an unintentional overlap with the subsequent senarmontite–valentinite transition, this argument does not explain the formation of cervantite, which should be an exothermic process at this temperature. Therefore, this data appears to

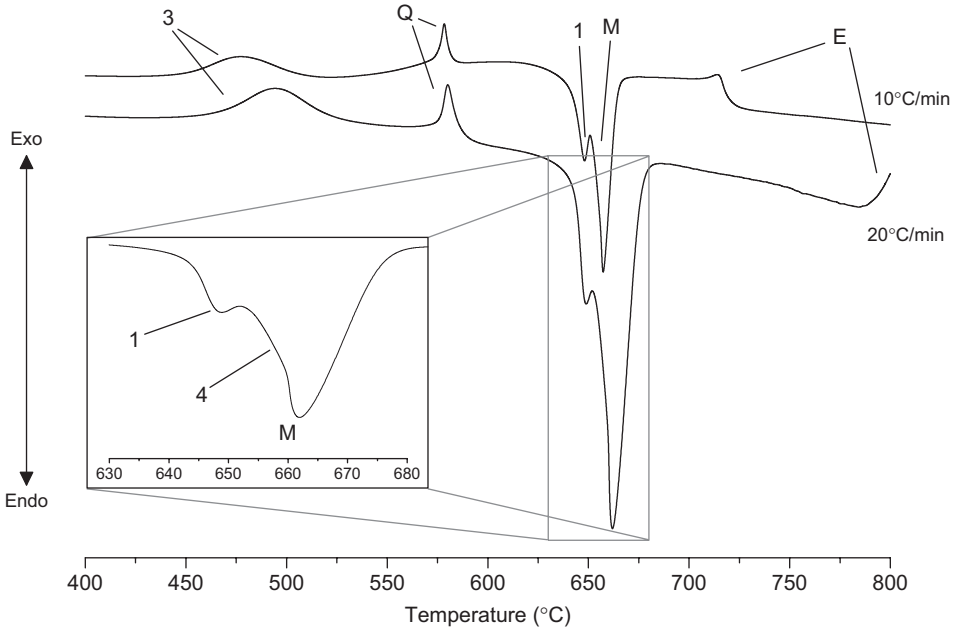

Fig. 8. Comparison of the DTA traces for the mechanically derived valentinite sample under flowing argon at heating rates of 10 and 20 °C/min. Peak labels: Q = α–β quartz transition; M = melting; E = end of volatilisation. Numbered peaks are discussed in more detail in the main text.

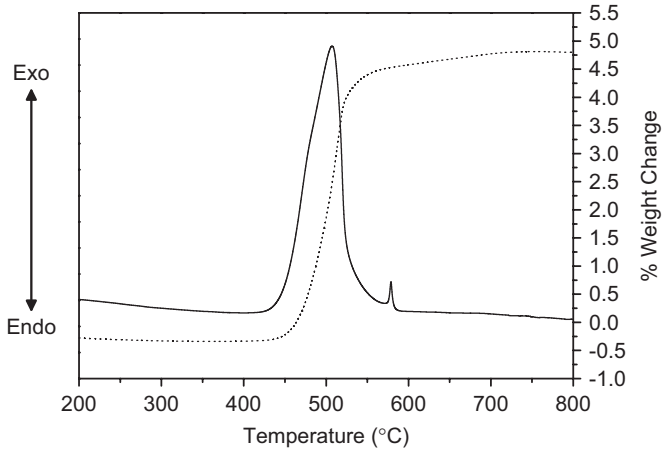

Fig. 9. DTA and TG data (solid and dotted lines, respectively) for the mechanically derived valentinite under air at 10 °C/min. Small peak at 575 °C is from the quartz transition.

suggest that event 1 is an example of the (partial) polymorphic phase transition, depressed by some mechanism, together with related oxidation from liberated oxygen. The following peak (labelled "P" in Fig. 3(a)) would then correspond to the remaining senarmontite converting to valentinite prior to melting.

Since all of the samples were heated under argon after a 30 min purge, the cervantite formation may imply that some oxygen remains in the local environment. However, if this were the case, oxidation would be expected to take place at a lower temperature, and there is no indication on the thermogravimetric curve (Fig. 3(b)) of an oxidation-related increase in mass. Another possible explanation for the formation of cervantite is that water is chemisorbed (as hydroxyl groups) and/or physically absorbed by the Sb_2O_3, and it is the resulting liberation of this on heating that provides the oxygen necessary for oxidation; due to the relative masses of H_2O and Sb_4O_6, any associated mass loss is difficult to detect amidst the sublimation effects. The presence of chemisorbed water may also be the cause of the depression of the partial phase transition.

Although event 1 was not immediately discernable on the heat-flow trace from milled senarmontite, the gradual onset of the phase transition, starting at 625 ± 3 °C, suggests that a depressed transition similar to that of the commercial senarmontite is also occurring in the finer-grain sample. A white residual mass was observed to remain in the crucible after each of the TG/DTA measurements on the crystalline Sb_2O_3 samples and, although too little remained for analysis, the absence of 100% mass loss at any point on the thermogravimetric curves suggests that this was cervantite—again, possibly the result of oxidation through thermal liberation of water in the samples.

4.1.2. Valentinite

Valentinite is thermodynamically unstable with respect to senarmontite below 600 °C [10] and, after passing through event 3 (shown in Fig. 8), XRD analysis of the material confirmed that conversion to senarmontite took place during this exothermic event. Under argon, there was no indication of cervantite formation through oxidation, which could have provided another explanation for the event (such as the presence of surface- or bulk-bound

water, as mentioned earlier for event 2). Under air, event 3 was obscured by oxidation.

Since the onset temperature, 445 ± 3 °C, for the valentinite–senarmontite phase transition is significantly lower than the value of 600 °C previously reported for commercial valentinite (which was presumably not prepared by mechanical milling), and because there is no evidence of other phases in the XRD analysis of the sample, it is plausible that the depression of the phase transition has occurred due to the method of sample preparation. The process of milling undertaken to produce the valentinite is likely to have formed crystallites under strain, which may be the source of the noticeably broadened peaks observed in XRD (Fig. 2(c)), and the additional energy present in the system as a result may have lowered the activation energy required for the transition to the thermodynamically favourable senarmontite. Alternatively, if the process is surface-nucleated, the smaller particle size produced by the milling may be the cause of the lowered transition. Since both strain-broadening and crystallite size contribute to XRD peak widths, it is not easy to estimate their relative importance.

At first sight, the DTA trace under argon for mechanically derived valentinite appears to show the senarmontite–valentinite phase transition at 615 ± 3 °C. However, expansion of the trace, as in the inset in Fig. 8, shows a second feature (labelled as "event 4") as a shoulder on the melting event, suggesting that a multi-stage polymorphic phase transition is occurring in the senarmontite derived from the valentinite sample. However, in this case absorbed water is unlikely to be the (sole) origin of the lowered valentinite–senarmontite transition, as there is no mention of this phenomenon in the literature (where, one can presume, some water-containing samples are likely to have been used) and because there was no oxidation observed in event 3 at lower temperature; it seems more plausible that the mechanical preparation of this valentinite sample is the primary cause of this effect.

To summarise, the senarmontite–valentinite transition in the commercial senarmontite and the milled valentinite samples have been seen to occur as a two-stage event, with onset temperatures of 615 ± 3 and 645 ± 3 °C for each stage. In the milled senarmontite, a single transition at 625 ± 3 °C was observed.

There is no evidence to support the value quoted by Roberts and Fenwick [4] of 570 ± 10 °C, and doubts expressed earlier about possible sulphur contamination (or other effects from attempted purification) in their sample would appear to be justified. Centers' assertion of 556 °C for the transition temperature [11] also appears to be in error.

Of the other temperatures reported in the literature (Table 1)—approximately, 606 ± 5 °C [7,9,12], 629 °C [5] and 640–655 °C [10]—a certain correlation can be seen with the values observed in this work. If the depression of the phase transition temperature is in fact related to varying amounts of bound water in Sb_2O_3, it is not unlikely that previous authors' observations are also based on insufficiently characterised samples, and that it is for this reason that the reported values differ so markedly from each other. The lack of mention of a two-stage transition event may be attributable to the use of less sensitive equipment, or to specifics of the mechanism as yet not discovered (it is worth noting, for example, that even at the sampling rate of 10 points per second used in this work, only a single transition peak was observed for the milled senarmontite sample). The onset of melting so soon after the transition is also a complicating factor.

4.2. Oxidation and volatilisation

There is evidence of sublimation in senarmontite in this work with samples beginning to noticeably lose mass at an increasing rate from 512 ± 5 °C under argon and from 465 ± 5 °C under air. Sublimation in the valentinite sample was not observed before it converted to senarmontite, an event that occurred at a lower than normal temperature (the valentinite–senarmontite transition has previously been reported to occur at 600 °C [10]).

4.2.1. Senarmontite

The oxidation temperature observed for the commercial and milled senarmontite samples, 531 ± 4 °C (Table 2), does not appear to correspond to any previously reported value. Variations in particle size between samples is not a likely cause, since the milled and commercial samples exhibited the same oxidation temperature and their mean particle sizes differ by a factor of two or more; other issues, such as the amount of oxygen in the local atmosphere and any bound water in the sample would seem more plausible explanations.

Comparison of the XRD spectra for the milled senarmontite before and after the relatively weak feature (event 2) observed under argon at 410 ± 5 °C shows that after the event the senarmontite peaks have narrowed appreciably (Fig. 5). This evidence, together with the shape of the peak in the DTA trace (Fig. 3(a)) suggests that the event is an order–disorder transformation (reducing the stress in the substance by slight re-arrangements of bond lengths and angles) and may be related to the oxygen stoichiometry of the system since, under flowing air, the feature is both more pronounced (Fig. 3(c)) and also occurs at a lower temperature (323 ± 3 °C). The cervantite formation under air (Fig. 6) may be explained by the atomic rearrangement providing an environment (due to short-term weakening or breaking of bonds) that allows some of the senarmontite to oxidise at a lower than normal temperature as the structure adjusts to reduce the overall stress in the system. The overall mass loss recorded over this event in the thermogravimetric data can be explained by Sb_2O_3 volatilisation, the onset of which has been depressed for the same reasons as oxidation.

Mass loss observed after bulk oxidation in the senarmontite samples agrees qualitatively with the literature

[5,8]. The overall mass loss under air was observed to be lower in the milled sample than in the commercial one (2.2% versus 8.6%)—this may be due to the loss of a greater amount of bound water in the latter, consistent with earlier arguments, or due to differing rates of volatilisation between the two Sb_2O_3 polymorphs (since the milled senarmontite was observed to convert to valentinite earlier than the commercial sample; rates of volatilisation could not be studied in this work due to the tendency of the mechanically derived valentinite to convert to senarmontite if unoxidised). Under argon the reverse is true, with the commercial senarmontite losing less mass due to earlier, possibly water-related, cervantite formation (as discussed earlier, and evinced in Fig. 4).

4.2.2. Valentinite

As previously reported [5,6,8] oxidation of valentinite occurred at a lower temperature than in the senarmontite

Table 2
The onset temperatures for thermal events and the mass changes in the Sb_2O_3 systems examined

Sample	Under argon			Under Air	
	Senarmontite–valentinite phase transition (±3 °C)	Melting temperature (±3 °C)	Total mass change (%)	Oxidation temperature (±3 °C)	Total mass change (%)
Commercial senarmontite	615 (643)	652	−89.7	532	−8.6
Milled senarmontite	625	650	−93.4	530	−2.2
Mechanically derived valentinite	616 (646)	654	−91.8	410	+4.6

Temperatures listed are for scan rates of 20 °C/min except for oxidation, where onset temperatures were more easily determined from 10 °C/min data. Two temperatures are given for the phase transitions where separate stages were identified (believed to be due to bound water). Also note that, under argon, the mechanically derived valentinite had fully converted to senarmontite prior to the onset of the events listed.

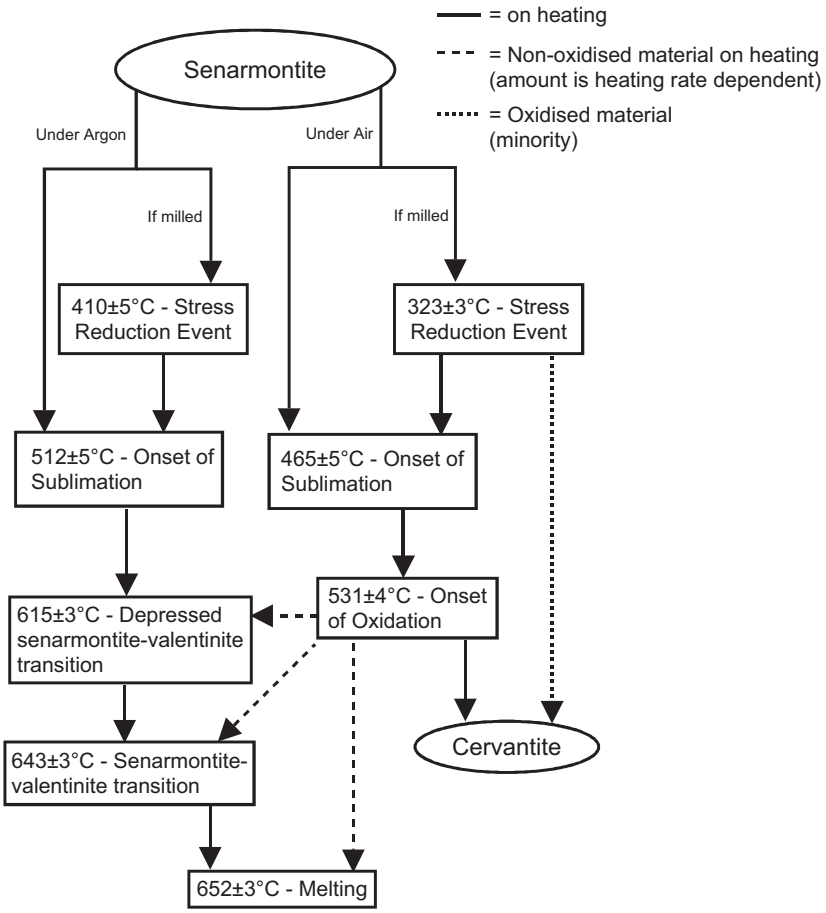

Fig. 10. Flow diagram summarising the thermal events occurring in α-Sb_2O_3 (senarmontite).

samples (the depressed valentinite–senarmontite transition observed in the mechanically derived valentinite under argon was apparently overridden by oxidation under air) and an overall mass increase of 4.75% was recorded (Fig. 9), instead of the mass loss noted by Golunski et al. [5]. This increase in mass contrasts with the loss observed after oxidation in the senarmontite samples and is probably a result of the earlier oxidation of valentinite to the stable cervantite form, preventing much of the original Sb_2O_3 from volatilising.

Under air, the mechanically derived valentinite sample began to oxidise at a temperature of $410\pm3\,^{\circ}C$ (Fig. 9), similar to that reported by Trofimov et al. [6]. This is significantly lower than the temperature reported by other authors [5,8] and it seems likely that the discrepancy is due to the smaller particle size to be expected of the valentinite prepared in this work.

4.3. Melting point

The melting point observed in the three samples, $652\pm5\,^{\circ}C$, is consistent with the temperature most commonly given for antimony trioxide. The overlap with the senarmontite–valentinite transition obscures any potential variation in the onset of melting with heating rate, as reported by Jones et al. [10]. The peak of the melting event shifts with increasing heating rate however (Fig. 7), as expected. The difficulty in distinguishing the melting onset from the preceding senarmontite–valentinite transition may account for the small variation in temperatures to be found in the literature.

5. Conclusions

Summary flow diagrams of the thermal events in the senarmontite and valentinite systems are shown in Figs. 10 and 11, respectively.

The senarmontite–valentinite transition has been observed to occur as a multi-stage event with the earlier stages apparently depressed by some mechanism; evidence of oxidation effects under argon suggests that the presence of surface- or bulk-bound water in the samples may be responsible.

Valentinite prepared through mechanical milling by the method outlined by Berry and Ren [15] converts to senarmontite at a much lower temperature ($445\pm3\,^{\circ}C$) than is normally quoted, probably due to either the small particle size or due to strain in the system as a result of the method of preparation. The process may still be advantageous for avoiding oxidation and volatilisation that occur during standard thermal preparations however.

Senarmontite milled by a less-energetic process than the above has been observed to exhibit an order–disorder transformation at $410\pm5\,^{\circ}C$ under argon ($323\pm3\,^{\circ}C$ under air) which reduces the strain due to milling; under air, a small amount of material also oxidises to cervantite during this process.

The oxidation temperature observed for senarmontite, $531\pm4\,^{\circ}C$, does not correspond to any previously reported value. The amount of oxygen in the local atmosphere and any bound water in the sample are possible explanations for these differences. Mechanically derived valentinite was observed to oxidise at $410\pm3\,^{\circ}C$, similar to the temperature reported previously by Trofimov et al. [6].

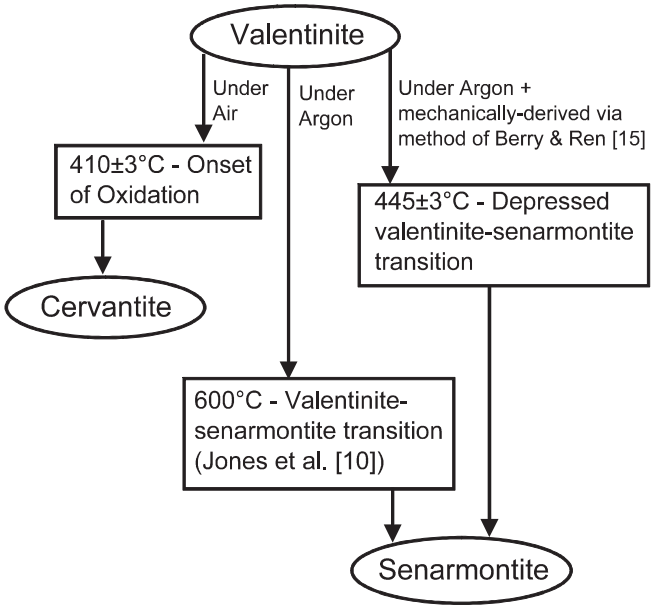

Fig. 11. Flow diagram summarising the thermal events occurring in β-Sb_2O_3 (valentinite).

Acknowledgments

The authors would like to thank Professor Frank Berry and Mr Xiaolin Ren at the Open University for their assistance in preparing valentinite by mechanical milling, and for the use of their equipment in doing so.

References

[1] C. Svensson, Acta Crystallogr. B 31 (1975) 2016–2018.
[2] C. Svensson, Acta Crystallogr. B 30 (1974) 458–461.
[3] G. Thornton, Acta Crystallogr. B 33 (1977) 1271–1273.
[4] E.J. Roberts, F. Fenwick, J. Am. Chem. Soc. 50 (1928) 2125–2147.
[5] S.E. Golunski, T.G. Nevell, M.I. Pope, Thermochim. Acta 51 (1981) 153–168.
[6] V.G. Trofimov, A.I. Sheinkman, G.V. Kleshchev, Izv. Vyssh. Uchebn. Zaved. Fiz. 3 (1973) 135–137.
[7] W.B. White, F. Dachille, R. Roy, Z. Kristallogr. 125 (1967) 450–458.
[8] C.A. Cody, L. DiCarlo, R.K. Darlington, Inorg. Chem. 18 (6) (1979) 1572–1576.
[9] Y.K. Agrawal, A.L. Shashimohan, A.B. Biswas, J. Therm. Anal. 7 (1975) 635–641.
[10] S.A. Jones, J. Fenerty, J. Pearce, Thermochim. Acta 114 (1987) 61–66.
[11] P.W. Centers, J. Solid State Chem. 72 (1988) 303–308.
[12] I. Barin, Thermochemical Data of Pure Substances, second ed., vol. 2., VCH, New York, 1993.
[13] P.S. Gopalakrishnan, H. Manohar, Pramana 3 (5) (1974) 277–285.
[14] S.E. Golunski, D. Jackson, Appl. Catal. 48 (1989) 123–135.
[15] F.J. Berry, X. Ren, J. Mater. Sci. 39 (2004) 1179–1183.